LUMIA Lab 2025-10-08

# AWM : Accurate Weight-Matrix Fingerprint for Large Language Models

Boyi Zeng<sup>1\*</sup>, Lin Chen<sup>1\*</sup>, Ziwei He<sup>2</sup>, Xinbing Wang<sup>3</sup>, Zhouhan Lin<sup>1,2‡</sup>

- <sup>1</sup> LUMIA Lab, School of Artificial Intelligence, Shanghai Jiao Tong University
- <sup>2</sup> Shanghai Innovation Institute <sup>3</sup> Shanghai Jiao Tong University
- boyizeng@sjtu.edu.cn lin.zhouhan@gmail.com \* Equal Contribution ‡ Corresponding Author.
- https://github.com/LUMIA-Group/AWM

Abstract Protecting the intellectual property of large language models (LLMs) is crucial, given the substantial resources required for their training. Consequently, there is an urgent need for both model owners and third parties to determine whether a suspect LLM is trained from scratch or derived from an existing base model. However, the intensive post-training processes that models typically undergo—such as supervised fine-tuning, extensive continued pretraining, reinforcement learning, multi-modal extension, pruning, and upcycling—pose significant challenges to reliable identification. In this work, we propose a training-free fingerprinting method based on weight matrices. We leverage the Linear Assignment Problem (LAP) and an unbiased Centered Kernel Alignment (CKA) similarity to neutralize the effects of parameter manipulations, yielding a highly robust and high-fidelity similarity metric. On a comprehensive testbed of 60 positive and 90 negative model pairs, our method demonstrates exceptional robustness against all six aforementioned post-training categories while exhibiting a near-zero risk of false positives. By achieving perfect scores on all classification metrics, our approach establishes a strong basis for reliable model lineage verification. Moreover, the entire computation completes within 30s on an NVIDIA 3090 GPU.

# 1. Introduction

Large language models (LLMs) have become foundational to many artificial intelligence applications. However, training an LLM from scratch demands substantial computational resources and vast amounts of data. Consequently, most open-source models are released under specific licenses (Kamath et al., 2025; Mesnard et al., 2024; Team et al., 2025; Touvron et al., 2023a) or require an application (BaiChuan-Inc, 2023; Grattafiori et al., 2024; Penedo et al., 2023; Team, 2023; Touvron et al., 2023b; Zhang et al., 2022; Zheng et al., 2023) and approval process to protect intellectual property. Despite these measures, some developers may circumvent such protections by wrapping or post-training existing base LLMs, then falsely claiming to have trained their own models. Recent controversies (pzc163 et al., 2024; Yoon et al., 2025) have underscored the urgent need

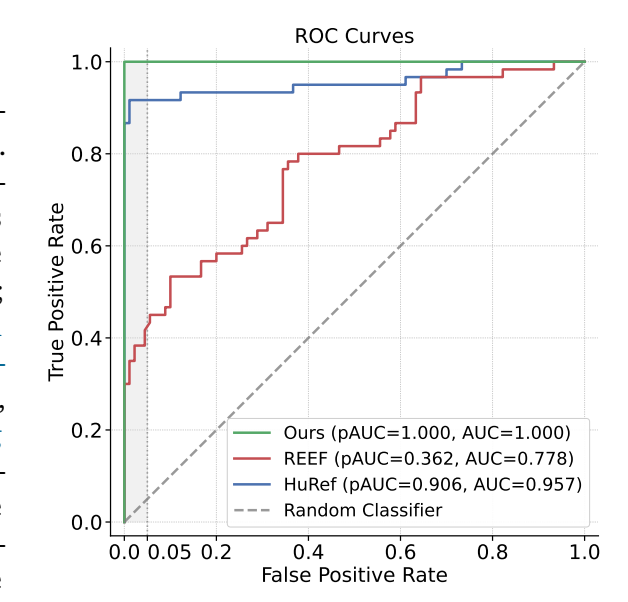


**Figure 1** | On 150 LLM pairs, our method achieves perfect AUC in distinguishing related and unrelated LLMs, outperforming baselines.

to determine whether a suspect model is genuinely trained from scratch or derived from an existing base model.

The core challenge lies in extracting a stable fingerprint to identify the true base model. This task is complicated by the fact that LLMs often undergo heavy post-training processes, such as supervised fine-tuning (SFT), extensive continued pretraining (Hui et al., 2024; Team et al., 2024), and reinforcement learning (RL). Furthermore, emerging techniques like extension to multimodal tasks, architectural pruning (Xia et al.), and upcycling (He et al., 2024) can drastically alter a model's parameters, outputs, and even its structure, posing substantial challenges for identification. Moreover, malicious actors might intentionally manipulate weight matrices through operations including scaling, permutation, pruning, and even rotation to obscure a model's origin.

Therefore, a practical fingerprinting method needs to satisfy the following critical conditions:

- Robustness against extensive post-training processes.
- Resilience to malicious weight manipulations such as scaling, pruning, permutation, and rotation.
- Performance Preservation, ensuring no degradation of the LLM's capabilities, as both users and manufacturers place a high premium on model performance.
- High Fidelity, possessing sufficient discriminative power and an extremely low false-positive rate to prevent false accusations of model theft.
- Computational Efficiency, remaining lightweight enough for comparisons given the immense parameter counts of modern LLMs.

A review of previous work reveals that existing methods often fail to meet one or more of these criteria. Watermarking techniques, for instance, embed identifiable signals via extra training (Peng et al., 2023; Xu et al., 2024), but this can degrade performance (Russinovich & Salem, 2024), may not survive aggressive post-training (Fernandez et al., 2024; Gubri et al., 2024), and must be applied before the model's release. Other existing fingerprinting methods either suffer from high false-positive rates (Zhang et al., 2025) or lack robustness against heavy post-training modifications like continued pretraining (Zeng et al., 2024), a limitation we confirm in our experiments.

In this work, we propose a novel approach that satisfies all the aforementioned requirements. Our method begins with an analysis of LLM weight manipulations. By leveraging the Linear Assignment Problem (LAP) and an unbiased Centered Kernel Alignment (CKA), we derive a similarity metric that is robust to all these manipulations. Our entire similarity computation completes within 30 seconds on a single NVIDIA 3090 GPU. Furthermore, our method is training-free and does not impair the LLM's performance.

We validate our approach on a comprehensive test set of 60 positive (base-offspring) and 90 negative (independent) model pairs. Compared to state-of-the-art methods such as HuRef and REEF, our approach achieves a much larger separation gap while maintaining a near-zero false-positive risk. Crucially, our method is the only one to prove robust against all tested forms of post-training: SFT, extensive continued pretraining (up to 5.5T tokens), reinforcement learning, multi-modal extension, pruning, and upcycling. On this 150-pair dataset, our method achieves a perfect Area Under the Curve (AUC), partial AUC (for False Positive Rate < 0.05), and True Positive Rate @ 1% False Positive Rate of 1.0, establishing a strong basis for reliable and robust model lineage verification.

# 2. Related Work

Model copyright protection methods fall into two main categories: watermarking and fingerprinting.

Watermarking. Watermarking methods typically involve finetuning models to inject backdoor

triggers that prompt the model to generate predefined content, or embedding watermarks directly into model weights for identification purposes. A substantial body of research has explored watermarking for smaller DNNs such as CNNs and BERT (Devlin et al., 2019), including encoding watermarks into model weights (Chen et al., 2019a; Liu et al., 2021; Uchida et al., 2017; Wang & Kerschbaum, 2021) and injecting triggers to produce specific outputs (Adi et al., 2018; Chen et al., 2019b; Guo & Potkonjak, 2018; Le Merrer et al., 2020). However, these methods are often task-specific and not well-suited for foundation LLMs. For watermarking LLMs, researchers have proposed various methods to inject watermarks for identification (Kirchenbauer et al., 2023; Li et al., 2023; Peng et al., 2023; Russinovich & Salem, 2024; Xu et al., 2024; Zhao et al., 2023). Nevertheless, these approaches inevitably compromise LLM performance and are not robust to extensive post-training.

Fingerprinting. Fingerprinting methods extract intrinsic model features as fingerprints for identification, without requiring additional training and thus without impacting model performance. For small DNNs, prior works (Lukas et al., 2019; Pan et al., 2022; Peng et al., 2022; Yang et al., 2022; Zhao et al., 2020) analyze model behaviors on preset test cases to construct fingerprints. For LLMs, HuRef (Zeng et al., 2024) is a classic weight-based fingerprinting method that derives invariant terms and computes similarities between them for model identification. However, it is not robust to extensive training. REEF (Zhang et al., 2025), from the perspective of representation, measures similarities between model representations, but suffers from a high false positive rate, which limits its practical use. To date, there is still a lack of fingerprinting methods for LLMs that are both robust to extensive training and exhibit a very low risk of false positives.

# 3. Preliminary

LLM Architecture Most Large Language Models (LLMs) follows a decoder-only Transformer architecture (Radford et al., 2018). The details of various LLMs may differ, yet the Transformer blocks are similar. In particular, a Transformer block in an LLM usually consists of residual connections (He et al., 2016), Root Mean Square Normalization (RMSNorm, Zhang & Sennrich (2019)), the selfattention mechanism (Lin et al., 2017), Rotary Position Embedding (RoPE, Su et al. (2024)), and a feed-forward network (FFN). We denote by  $W_A$  the set of an L-layered LLM A's weights, and  $\mathbb{W}_{A, \text{partial}} = \{W_{A, \text{emb}}\} \bigcup_{l=1}^{L} \{W_{A, i}^{(l)} \mid i \in \{Q, K\}\} \text{ the set of word embeddings and } Q, K \text{ matrices, where}$  $W_{A,\text{emb}}$  is the word embeddings and  $W_{A,Q}^{(l)}, W_{A,K}^{(l)}$  are the Q, K matrices at the l-th layer. We defer the rest of the notations to Appendix A.1.

Central Kernel Alignment (CKA) Proposed in Kornblith et al. (2019), CKA is a similarity detection method (Zhang et al., 2025) based on Hilbert-Schmidt Independence Criterion (HSIC, Gretton et al. (2005)). It is invariant to column-wise orthogonal transformations and constant multiplications:

**Theorem 3.1.** For any input matrices  $X_1 \in \mathbb{R}^{m \times n_1}$ ,  $X_2 \in \mathbb{R}^{m \times n_2}$ , any orthogonal transformations  $U_1 \in \mathbb{R}^{n_1 \times n_1}, U_2 \in \mathbb{R}^{n_2 \times n_2}$ , any non-zero constants  $c_1, c_2 \in \mathbb{R}$ ,

$$CKA(X_1, X_2) = CKA(c_1X_1U_1, c_2X_2U_2).$$
 (1)

Even with semi-orthogonal  $U_1$  and  $U_2$  where  $U_1 \in \mathbb{R}^{n_1 \times n_1'}$ ,  $U_2 \in \mathbb{R}^{n_2 \times n_2'}$ ,  $n_1 > n_1'$ ,  $n_2 > n_2'$ , CKA still preserves input similarity to some extent (Chun et al., 2025; Kang et al., 2025). Nevertheless, the standard HSIC estimator converges at rate  $1/\sqrt{m}$  and shows finite-sample bias (Gretton et al., 2005; Murphy et al., 2024). To this end, an unbiased version (Song et al., 2007) is proposed and extends the value of CKA from [0, 1] to [-1, 1]. Additionally, linear kernels are often selected in CKA due to their computational efficiency and similar performance to other kernels (Kornblith et al., 2019). We give the formal definition of CKA in Appendix A.2, and the proof of Theorem 3.1 in Appendix B.1.

# 4. Manipulations on An Open-Source LLM

## 4.1. Problem Definition

Weights of an open-source LLM are often inherited, but unclaimed inheritance invites manipulations. Although the source code may not explicitly reveal these manipulations, the weights are vulnerable to modifications that leave no trace in code (e.g., post-hoc matrix multiplications to produce new weights), and they can even be altered to evade independence tests. To enable detection on model weights, we first formalize the plausible manipulation forms.

**Definition 4.1** (LLM Weight Manipulations). Let A and B be two open-source LLMs with the same number of layers L, and  $\mathbb{W}_A$ ,  $\mathbb{W}_B$  denote the sets of matrix weights for A and B respectively. Then, if B manipulates A, the manipulations on  $W_{A,partial}$  are

$$W_{B,i}^{(l)} = L_{B,i}^{(l)} W_{A,i}^{(l)} R_{B,i}^{(l)} + E_{B,i}^{(l)} \quad for \ all \ 1 \le l \le L \ and \ i \in \{Q,K\}$$
 (2)

$$W_{B.emb} = W_{A.emb} R_{B.emb} + E_{B.emb} \tag{3}$$

where L and R are row-wise and column-wise transformation matrices, and E is the error term. The learnable weights in RMSNorm are also changed correspondingly.

We omit the row-wise transform on word embeddings,  $L_{B,emb}$ , since each row of  $W_{A,emb}$  represents a token and mixed token representations are hard to be faithfully recovered in the calculation of attention scores. We further assume that the suspicious and manipulated models produce similar (or identical) outputs to be consistent with the goal of reusing base model performance. This assumption induces constraints on the transformation matrices and, in turn, enables detection via weight-matrix similarity tests. We first develop a fine-grained view of the constraints on  $W_{A,partial}$  in what follows.

# 4.2. Residual Connections: Passing Manipulations Forward

A Transformer block consists of multiple components linked by residual connections. If one component takes input X, the next receives Y = X + f(X), so any manipulation T on X must be recovered within the component to propagate as the next input (Zeng et al., 2024). This propagation also depends on the constituent functions of the component, which either commute with the manipulation to recover it or remain invariant and absorb it. We formalize this in the following:

**Proposition 4.2** (Proof in Appendix B.2). Let  $f = f_n \circ \cdots \circ f_1$  be a component in Transformer and let T be a manipulation in the input. If for every  $k \in \{1, ..., n\}$ ,  $T \circ f_k = f_k \circ T$ , then  $f \circ T = T \circ f$ , i.e. the manipulation propagates through constituent functions of a component.

Compared to Zeng et al. (2024), Proposition 4.2 shows that residual connections are more vulnerable under a component-wise view, since constituent functions can propagate manipulations in various ways. However, nonlinearities of the functions, especially those within the self-attention mechanism, pose constraints for manipulations on both inputs and weights. We next split the selfattention mechanism into two constituent functions, RMSNorm and attention (see Definition A.4), and show how these effects arise and are constrained these two functions with a focus on RMSNorm, RoPE and attention scores.

## 4.3. RMSNorm: A Constraint on Embedding Manipulations

Any input to the self-attention mechanism, including word embeddings and hidden states, first go through RMSNorm. However, RMSNorm can facilitate potential manipulations on inputs, because it commutes with certain transformations  $R_{B, \text{emb}}$  of the embeddings:

**Theorem 4.3.** Let models A and B share the same  $^1$  architecture. Let  $c \neq 0$  be a scalar, P be a (partial) permutation matrix, and D be a signature matrix. Then,  $R_{B.emb} = cPD$  can be recovered after RMSNorm in model B if related RMSNorm parameters are adjusted.

Theorem 4.3 indicates that RMSNorm is susceptible to embedding manipulations composed of constant multiplications, permutations and sign flips. On the other hand, other manipulations on word embeddings are generally neither commutative with RMSNorm nor invariant to it, which potentially brings a constraint to manipulations. We provide a proof for Theorem 4.3 in Appendix B.3, along with a discussion on other manipulations on word embeddings.

# 4.4. RoPE and Attention Scores: Boundaries for Q/K Manipulations

After RMSNorm, inputs are fed into attention score calculations. The nonlinearity here, particularly in the softmax and RoPE functions, poses a barrier for manipulations on inputs to pass through. Hence, we follow Zeng et al. (2024) to assume that input manipulations does not change the value of attention scores. The manipulations on Q,K matrices are thus constrained under this assumption.

**Theorem 4.4.** The manipulations on Q.K matrices at layer l can be categorized into

- 1. Input-related ones, passed by RMSNorm:  $W_{B,i}^{(l)}=c^{-1}W_{A,i}^{(l)}PD$ , for  $i\in\{Q,K\}$ ; 2. RoPE-related ones:  $W_{B,i}^{(l)}=U_{B,i}^{(l)}W_{A,i}^{(l)}$ , for  $i\in\{Q,K\}$ ;

where  $\boldsymbol{U}_{B,i}^{(l)}$  are special orthogonal matrices that keep RoPE results.

A proof for Theorem 4.4 is provided in Appendix B.4, where we also show how manipulations on inputs are recovered after V, O matrices to satisfy Proposition 4.2. These manipulations preserve the attention score values of model A in the suspicious model B. However, they can greatly change the weights of the original model A, bringing difficulty to the development of detection methods.

## 4.5. Potential Attacks

Combining Theorem 4.3 and Theorem 4.4, the admissible manipulations on  $W_{A,partial}$  (word embeddings and Q, K matrices) in Definition 4.1 are restricted to

$$W_{B,i}^{(l)\top} = c^{-1} D^{\top} P^{\top} W_{A,i}^{(l)\top} U_{B,i}^{(l)\top} + E_{B,i}^{(l)\top}, \quad 1 \le l \le L, \quad i \in \{Q, K\},$$
(4)

$$W_{B,\text{emb}} = c W_{A,\text{emb}} PD + E_{B,\text{emb}}.$$
 (5)

Here E collects post-training, continual pre-training, pruning, upcycling, multimodal adaptation, or related adjustments. The nonlinear usage of  $W_{A,partial}$ , especially through the Q, K matrices, substantially limits manipulation complexity. Consequently, checking similarity between  $W_{A,partial}$  and  $W_{B,partial}$ is typically sufficient for detection. The remaining avenues targeting  $\mathbb{WA}/\mathbb{W}_{A,partial}$  are deferred to Appendix B.5, where we also discuss how such transformations can recover Transformer block outputs in light of Proposition 4.2.

# 5. Methodology

Building on Theorem 4.3 and Theorem 4.4, we propose a two-stage procedure in 1: (i) extract P and D from the word embeddings; (ii) assess cross-model similarity by comparing the Q and K matrices. This design achieves fast, reliable discrimination with minimal computation.

<sup>&</sup>lt;sup>1</sup>The conclusions generalize to models with different number of layers (possibly a result of pruning). See Appendix B.3

# Algorithm 1 LAP-Enhanced Unbiased Central Kernel Alignment (UCKA) Similarity Detection

```
1: Given two L^2-layered LLMs A, B and their weight matrices \mathbb{W}_{A,\text{partial}}, \mathbb{W}_{B,\text{partial}}.
 2: Let I = Vocab(A) \cap Vocab(B), and m' = |I|.
 3: Let W_{A,\text{shared-emb}} = W_{A,\text{emb}}[I,:] and W_{B,\text{shared-emb}} = W_{B,\text{emb}}[I,:].
 4: Build the cosine similarity matrix C with C_{k,l} = \frac{\langle (W_{A,\text{shared-emb}})_{:,k}, (W_{B,\text{shared-emb}})_{:,l} \rangle}{\|(W_{A,\text{shared-emb}})_{:,k}\| \|(W_{B,\text{shared-emb}})_{:,l}\|}
 5: Construct the permutation and signature matrices P, D via LAP:
            Find a permutation \pi maximizing \sum_{k} |C_{k,\pi(k)}| with the Hungarian algorithm.
 6:
           For each column k, set s_k = \text{sign}(C_{k,\pi(k)}).
 7:
            Set P_{k,\pi(k)} = 1 for every k, set D = \text{diag}(s_1, s_2, \dots, s_k, \dots).
           s_{Q}^{(l)} = \text{UCKA}\Big(D^{\top}P^{\top}W_{A,Q}^{(l)\top}, W_{B,Q}^{(l)\top}\Big), s_{K}^{(l)} = \text{UCKA}\Big(D^{\top}P^{\top}W_{A,K}^{(l)\top}, W_{B,K}^{(l)}\Big)
10:
12: return \sum_{l=1}^{L} (|s_Q^{(l)}| + |s_K^{(l)}|)/2L
```

Extracting the Permutation and Signature from Word Embeddings A key property of  $R_{B,\text{emb}}$  is that the permutation and signature matrices may appear in either order: both  $R_{B,\mathrm{emb}} = cPD$  and  $R_{B,\text{emb}} = cDP$  are possible. However, any product DP can be rewritten as P'D' for some permutations P' and signature matrices D'. Hence it suffices to recover a canonical PD from the embeddings. We cast this as a Linear Assignment Problem (LAP; Burkard & Cela (1999)) solved by the Hungarian algorithm (Kuhn, 1955), which is invariant to any nonzero scalar factor. Specifically, we first restrict to the shared vocabulary and form the matrix of absolute cosine similarities between the columns of  $W_{A,\text{emb}}$  and  $W_{B,\text{emb}}$ . Then, LAP is applied to obtain the permutation P. Next, we use the signs of the cosine similarities at the matched pairs to reconstruct the signature matrix D. This approach effectively reconstruct corresponding transformations due to its low demand of additional parameters in the detection process.

Robust Recovery of Weight Similarities Despite accounting for permutation and signature manipulations, the orthogonal transformations  $U_{Bi}^{(l)}$  remain challenging. They introduce a substantial nuisance parameter burden: if  $W_{A,i}^{(l)} \in \mathbb{R}^{d \times n}$ , then orthogonal  $U_{B,i}^{(l)} \in \mathbb{R}^{d \times d}$  contributes  $d^2$  parameters, which is prohibitive when  $d \approx n$  and can undermine robustness by adding parameters to detections (Simmons et al., 2011). We therefore use Central Kernel Alignment (CKA) as a parameter-free similarity metric: by Theorem 3.1, CKA is invariant to orthogonal transforms and constant rescaling. While this invariance does not extend to semi-orthogonal  $U_{B,i}^{(l)}$  (e.g., induced by pruning), CKA remains effective to a meaningful extent in such cases, relieving the need to explicitly reconstruct  $U_{B,i}^{(l)}$ . To further mitigate biases (Gretton et al., 2005; Murphy et al., 2024), we adopt the unbiased variant (Song et al., 2007), termed UCKA (see Appendix A.2).

# 6. Experiments

In this section, we present a series of experiments designed to rigorously evaluate our proposed model fingerprinting method. We begin in subsection 6.1 by verifying its fundamental ability to distinguish between derived (offspring) and independent models. Next, in subsection 6.2, we assess the critical risk of false positives by comparing its performance on 90 pairs of independent models against two state-of-the-art baselines, HuRef and REEF. In subsection 6.3, we test the method's robustness against

<sup>&</sup>lt;sup>2</sup>For LLMs with differing layer counts  $(L_A, L_B)$ , e.g., from layer pruning, we find the optimal layer pairing by solving the LAP on an  $L_A \times L_B$  matrix of layer-wise similarities before calculating overall similarity.

**Table 1** | Similarity (%) of various LLMs to LLaMA2-7B and LLaMA2-13B base models. Offspring models consistently show high similarity scores (light red), while independent models have negligible similarity (light green), demonstrating the method's discriminative power.

Base	Model:	LLaMA2-7B		Base Model: LLaMA2-13B				
Offspring	Offspring Sim Independent Sim		Offspring	Sim	Independent	Sim		
WizardMath-7b	99.99	Baichuan-7b	0.58	Selfrag_llama2_13b	99.99	Baichuan-13b	0.17	
Selfrag_7b	99.98	Mistral-7b	0.63	Nous-Hermes-13b	99.98	Baichuan2-13b	0.23	
Vicuna-7b	99.95	OLMo-7b	0.46	Llama2-13b-orca	99.98	OLMo2-13b	0.21	
Llama2-7b-Chat	99.93	Qwen-7b	0.19	Vicuna-13b	99.93	Qwen-14b	0.20	
Finance-7b	99.93	InternLM-7b	0.43	Llama2-13b-Chat	99.92	Qwen3-14b	0.41	
Llama2-7b-32K	99.88	MPT-7b	0.04	Firefly-llama2-13b	99.81	Jais-13b	0.03	
Guanaco-7b	99.80	LLaMA-7b	0.81	Llama2-koen-13b	97.76	LLaMA-13b	0.74	
Llama2-ko-7b	96.79	OpenLlama-7b	0.71	Llama2-13b-Estopia	96.60	OpenLlama-13b	0.51	

a wide array of common post-training modifications using a comprehensive suite of 60 offspring models. Finally, in subsection 6.4, we provide an overall performance comparison, leveraging ROC curves and other metrics to demonstrate our method's superior discriminative power.

Baselines. We compare our method against two advanced baselines: the weight-based method HuRef (Zeng et al., 2024), and the representation-based method REEF (Zhang et al., 2025).

#### 6.1. Effectiveness Verification

We first established our method's core effectiveness in identifying model lineage. We collected eight offspring models for both LLaMA2-7B and LLaMA2-13B, alongside eight independent models for each size. We then calculated the similarity between the base model and these two groups.

As shown in Table 1, the results demonstrate a clear distinction. Offspring models exhibited exceptionally high similarity to their respective base models, whereas the similarity scores between independent models were negligible, forming a strong basis for intellectual property protection.

## 6.2. False Positive Risk Evaluation on 90 Unrelated Pairs

A critical requirement for any reliable fingerprinting method is an extremely low false positive rate. To evaluate this risk, we collected 10 independent 7B LLMs and 10 independent 13B LLMs, forming 45 unique pairs for each size. We then computed the pairwise similarity (%) for all 90 pairs using our method and compared the results with those from REEF and HuRef.

The heatmaps in Figure 2 illustrate our method's superior performance in avoiding false positives. For independent pairs, our method yielded mean similarity scores of just 0.49 (7B) and 0.26 (13B). These scores are nearly an order of magnitude lower than HuRef (means of 3.56 and 2.17) and two orders of magnitude lower than REEF (means of 42.47 and 47.44).

Notably, REEF frequently produces dangerously high similarity scores for unrelated models, with many pairs exceeding 80 and some even surpassing 95. Such high values could easily lead to false accusations of model theft. In contrast, the maximum similarity scores for our method were merely 1.5 (7B) and 0.8 (13B), reaffirming its significantly lower risk of false positives.



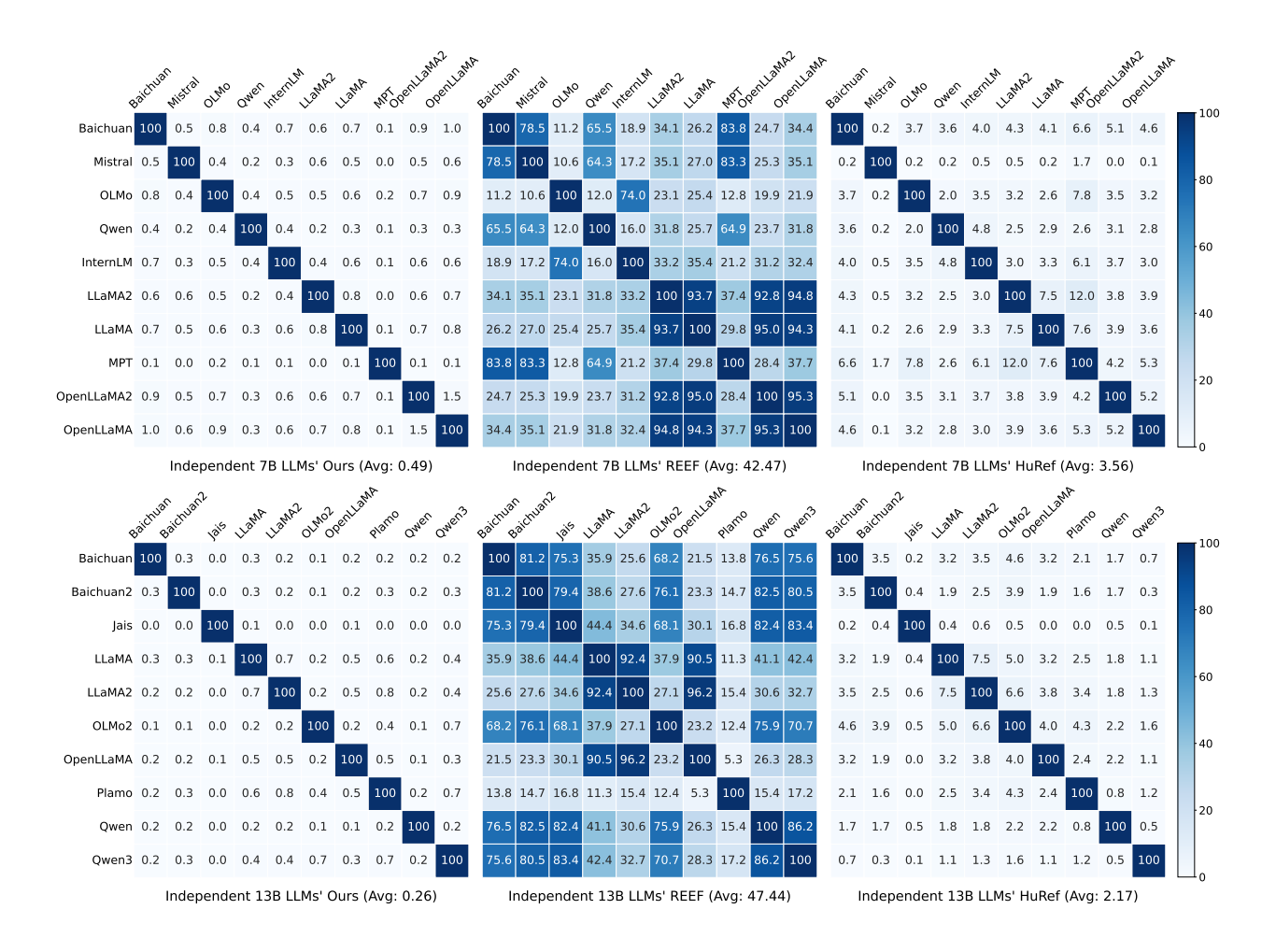


Figure 2 | Pairwise similarity (%) heatmaps for independent 7B (top row) and 13B (bottom row) LLMs. The columns compare our proposed method against two baselines, REEF and HuRef. Our method consistently yields near-zero similarity scores for all independent model pairs, indicating a significantly lower risk of false positives. In contrast, REEF often produces high similarity scores (> 80), which could easily lead to false accusations of model theft.

## 6.3. Robustness Verification on 60 Offspring Models

Base LLMs often undergo substantial post-training modifications, including SFT, continued pretraining, reinforcement learning (RL), pruning, upcycling, and multi-modal adaptation. These processes can significantly alter model parameters, making robustness a critical attribute for any fingerprinting technique. To rigorously evaluate our method's robustness, we curated a diverse test suite of 60 positive pairs, each consisting of a base model and a derived offspring model. This suite includes 10 pairs for each of the six modification categories listed above.

The effectiveness of a fingerprinting method hinges on its ability to distinguish between related (positive) and unrelated (negative) pairs. However, absolute similarity scores (%) can be misleading. A method yielding scores of 10 for a positive pair and 0.1 for negative pairs is far more discriminative than one producing scores of 90 and 40. To accurately measure the discriminative power, we must quantify how statistically different a positive pair's similarity is from the distribution of negative pairs. For this, we use the absolute Z-score  $(|Z|)^3$ . This metric measures how many standard deviations a

<sup>&</sup>lt;sup>3</sup>In this context, the absolute Z-score is mathematically equivalent to the Mahalanobis distance.



**Table 2** | Absolute Z-scores (↑) of positive samples for HuRef, REEF, and our method. The full names of abbreviations are provided in Appendix C.

					SFT					
Base	Llama2-13B						3			
Offspring	Vicuna	Finance	Selfrag	32K	Wizard	Guanaco	Vicuna	Hermes	Estopia	Firefly
HuRef	44.22	44.20	44.47	44.22	44.51	44.12	44.25	44.48	43.09	44.51
REEF	1.95	1.94	1.95	1.88	1.95	1.94	1.94	1.95	1.91	1.95
Ours	355.09	355.02	355.20	354.84	355.23	354.55	355.02	355.20	343.14	354.59
				Con	tinue Pret	rain				
Base		Llama2-7B	Gemma -2B		Gemma -7B	_	en2.5 7B	Qwen2 -7B	Llama	2-70B
Offspring	Llemma (700B)	Code (520B)	Python (620B)	Code (500B)	Code (500B)	Math (1T)	Coder (5.5T)	Math (700B)	Code (520B)	Python (620B)
HuRef	8.15	9.41	9.19	28.97	39.51	0.28	0.57	1.01	3.43	2.78
REEF	1.66	1.31	1.77	0.32	1.52	1.04	1.29	1.09	1.93	1.92
Ours	250.32	250.78	253.28	198.18	268.72	177.57	135.17	183.49	241.12	232.92
					Upcycling	5				
Base	Mistral -7B	Llama3 -8B			Llan	na2-7B			Qwen -1.8B	Minicpm -2B
Offspring	Mixtral	MoE v2	MoE4	MoE 3B	MoE2	MoE3B -SFT	MoE2 -SFT	MoE4 -SFT	Qwen1.5 MoE	Minicpm MoE
HuRef	7.97	42.50	24.58	21.59	24.91	21.59	24.91	24.58	4.03	11.39
REEF	1.47	0.47	0.64	0.64	0.62	0.63	0.63	0.62	0.57	1.49
Ours	239.01	332.12	332.23	326.49	332.12	326.49	332.12	332.23	173.36	150.15
				N	Iulti Moda	al				
Base	Llama2-7B		Qwen2 -7B	( IW/Ph_ / B			Qwen2.5 -7B	Qwen2.5 -3B	Llama3 -8B	Llama2 -13B
Offspring	LLaVA	Video	VL	Audio	Audio2	VL	VL	VL	Next	LLaVA
HuRef	44.06	44.03	39.94	38.79	21.59	37.41	24.28	23.95	44.30	44.09
REEF	0.40	0.36	0.84	0.19	0.45	0.77	0.48	0.61	0.26	0.07
Ours	354.98	354.98	342.72	339.86	317.97	336.55	290.08	298.46	355.05	354.91
					RL					
Base	Open- llama3B	Qwen2.5 -7B	Qwen2.5 -1.5B	Mixtral	Mist	ral-7B	Minicpm -2B	Qwen3 -4B	Chatglm -6B	Llama3 -8B
Offspring	RLHF	Reason	Zero	DPO	DPO	Dolphin	DPO	GRPO	RLHF	DPO
HuRef	44.52	44.58	44.58	44.57	44.53	44.54	44.58	44.58	44.58	44.52
REEF	1.94	1.93	1.94	1.75	1.48	1.21	1.92	1.78	1.96	1.96
Ours	355.23	355.27	355.27	355.23	355.23	355.23	355.27	355.27	355.27	355.23
Pruning										
Base	Llama-		-3-8B	3-8B			Llama2-7B			
Offspring	Minitron -Depth	Minitron -Width	Llama3 -1B	Llama3 -3B	Sheared 2.7B-P	Sheared 2.7B-S	Sheared 2.7B	Sheared 1.3B-P	Sheared 1.3B	Sheared 1.3B-S
HuRef	28.29	22.23	0.33	0.73	22.88	16.00	15.86	10.06	7.64	7.64
REEF	0.52	0.53	1.15	0.92	1.75	1.78	1.77	1.80	1.79	1.79
Ours	344.07	343.00	12.14	106.29	328.81	312.44	312.80	317.79	297.50	297.50



Table 3 | Detailed performance comparison of fingerprinting methods across various post-training techniques. Our method consistently achieves perfect scores (1.0) on all classification metrics (AUC, pAUC, TPR@1%FPR) and maintains a significantly larger separation margin (|Z|) across all scenarios. CPT: Continual Pre-Training, UP: Upcycling, MM: Multi-modal, PR: Pruning.

Method	Metric	SFT	CPT	UP	MM	RL	PR	All
	$\overline{ Z } \uparrow$	43.748	10.331	20.805	36.244	44.559	13.166	28.142
HuRef	AUC ↑	1.000	0.879	0.999	1.000	1.000	0.866	0.957
Hukei	pAUC ↑	1.000	0.656	0.978	1.000	1.000	0.800	0.906
	TPR@1%FPR↑	1.000	0.500	0.900	1.000	1.000	0.800	0.867
	$\overline{ Z } \uparrow$	1.936	1.384	0.777	0.443	1.788	1.381	1.285
DEEE	AUC ↑	1.000	0.857	0.508	0.648	0.963	0.692	0.778
REEF	pAUC ↑	1.000	0.211	0.000	0.000	0.658	0.300	0.362
	TPR@1%FPR↑	1.000	0.200	0.000	0.000	0.600	0.000	0.300
	$\overline{ Z } \uparrow$	353.788	219.155	287.634	334.556	355.250	267.233	302.936
Ours	AUC ↑	1.000	1.000	1.000	1.000	1.000	1.000	1.000
	pAUC ↑	1.000	1.000	1.000	1.000	1.000	1.000	1.000
	TPR@1%FPR↑	1.000	1.000	1.000	1.000	1.000	1.000	1.000

positive pair's similarity is from the mean of the negative pairs' similarities. A larger |Z| indicates that the positive pair is more likely to be a statistical outlier relative to the population of unrelated pairs and thus more highly separable.

The results, presented in Table 2, highlight the superior robustness of our method. HuRef loses effectiveness under heavy modifications like extensive continued pretraining (e.g., its |Z| drops to 0.57 for Qwen2.5-coder). REEF consistently yields low |Z|, often below 2.0, indicating poor separability. In stark contrast, our method maintains remarkably high |Z| across all 60 positive pairs, demonstrating its resilience against a wide array of demanding post-training modifications.

#### 6.4. Overall Evaluation

To synthesize our findings, we conducted a comprehensive evaluation against HuRef and REEF using the full dataset of 60 positive and 90 negative model pairs.

As illustrated in Figure 1, our method demonstrates vastly superior performance. The Receiver Operating Characteristic (ROC) curve (left) shows that our method achieves a perfect Area Under the Curve (AUC) of 1.0, indicating flawless discrimination. This starkly outperforms both HuRef (AUC = 0.957) and REEF (AUC = 0.778).

In practical applications, preventing false accusations of model theft is paramount, making performance at a very low False Positive Rate (FPR) essential. We therefore employ two stricter metrics: the partial AUC for FPR < 0.05 (pAUC) and the True Positive Rate at a 1% FPR (TPR@1%FPR).

Table 3 details the performance breakdown across post-training techniques. Our method consistently achieves perfect scores (1.0) on all classification metrics (AUC, pAUC, and TPR@1%FPR) across all categories. In contrast, the baseline methods show significant limitations. REEF's performance collapses in several scenarios, with pAUC and TPR@1%FPR scores falling to 0.0 for Upcycling and Multi-modal. HuRef also shows vulnerability, with its TPR@1%FPR dropping to 0.500 under Continual Pre-Training. Our method's perfect classification scores, combined with its substantially larger average absolute Z-score (|Z|), underscore its superior robustness and reliability.



# 7. Conclusions

In this paper, we propose a training-free fingerprinting method for LLM identification. Our approach does not impair LLM's general capability while exhibiting robustness against fine-tuning, extensive continued pretraining, reinforcement learning, multimodal extension, pruning, and upcycling, and simultaneously avoids the risk of false positives. Experiments on a testbed comprising 150 pairs of LLMs demonstrate the effectiveness of our method.

# Acknowledgement

This work is sponsored by the National Key Research and Development Program of China (No. 2023ZD0121402) and the National Natural Science Foundation of China (NSFC) grant (No.62576211).

# References

- Yossi Adi, Carsten Baum, Moustapha Cisse, Benny Pinkas, and Joseph Keshet. Turning your weakness into a strength: Watermarking deep neural networks by backdooring. In 27th USENIX Security Symposium (USENIX Security 18), pp. 1615–1631, 2018.
- BaiChuan-Inc. https://github.com/baichuan-inc/Baichuan-7B, 2023.
- Rainer E Burkard and Eranda Cela. Linear assignment problems and extensions. In Handbook of combinatorial optimization: Supplement volume A, pp. 75-149. Springer, 1999.
- Huili Chen, Bita Darvish Rouhani, Cheng Fu, Jishen Zhao, and Farinaz Koushanfar. Deepmarks: A secure fingerprinting framework for digital rights management of deep learning models. In Proceedings of the 2019 on International Conference on Multimedia Retrieval, pp. 105–113, 2019a.
- Huili Chen, Bita Darvish Rouhani, and Farinaz Koushanfar. Blackmarks: Blackbox multibit watermarking for deep neural networks. arXiv preprint arXiv:1904.00344, 2019b.
- Chanwoo Chun, Abdulkadir Canatar, SueYeon Chung, and Daniel D Lee. Estimating neural representation alignment from sparsely sampled inputs and features. arXiv preprint arXiv:2502.15104, 2025.
- Jacob Devlin, Ming-Wei Chang, Kenton Lee, and Kristina Toutanova. Bert: Pre-training of deep bidirectional transformers for language understanding. In Proceedings of the 2019 conference of the North American chapter of the association for computational linguistics: human language technologies, volume 1 (long and short papers), pp. 4171–4186, 2019.
- Pierre Fernandez, Guillaume Couairon, Teddy Furon, and Matthijs Douze. Functional invariants to watermark large transformers. In ICASSP 2024-2024 IEEE International Conference on Acoustics, Speech and Signal Processing (ICASSP), pp. 4815–4819. IEEE, 2024.
- Aaron Grattafiori, Abhimanyu Dubey, Abhinav Jauhri, Abhinav Pandey, Abhishek Kadian, Ahmad Al-Dahle, Aiesha Letman, Akhil Mathur, Alan Schelten, Alex Vaughan, et al. The llama 3 herd of models. arXiv preprint arXiv:2407.21783, 2024.
- Arthur Gretton, Olivier Bousquet, Alex Smola, and Bernhard Schölkopf. Measuring statistical dependence with hilbert-schmidt norms. In International conference on algorithmic learning theory, pp. 63–77. Springer, 2005.
- Martin Gubri, Dennis Ulmer, Hwaran Lee, Sangdoo Yun, and Seong Joon Oh. Trap: Targeted random adversarial prompt honeypot for black-box identification. arXiv preprint arXiv:2402.12991, 2024.
- Jia Guo and Miodrag Potkonjak. Watermarking deep neural networks for embedded systems. In 2018 IEEE/ACM International Conference on Computer-Aided Design (ICCAD), pp. 1–8. IEEE, 2018.
- Ethan He, Abhinav Khattar, Ryan Prenger, Vijay Korthikanti, Zijie Yan, Tong Liu, Shiqing Fan, Ashwath Aithal, Mohammad Shoeybi, and Bryan Catanzaro. Upcycling large language models into mixture of experts. arXiv preprint arXiv:2410.07524, 2024.
- Kaiming He, Xiangyu Zhang, Shaoqing Ren, and Jian Sun. Deep residual learning for image recognition. In Proceedings of the IEEE conference on computer vision and pattern recognition, pp. 770–778, 2016.
- Binyuan Hui, Jian Yang, Zeyu Cui, Jiaxi Yang, Dayiheng Liu, Lei Zhang, Tianyu Liu, Jiajun Zhang, Bowen Yu, Keming Lu, et al. Qwen2. 5-coder technical report. arXiv preprint arXiv:2409.12186, 2024.

- Aishwarya Kamath, Johan Ferret, Shreya Pathak, Nino Vieillard, Ramona Merhej, Sarah Perrin, Tatiana Matejovicova, Alexandre Ramé, Morgane Rivière, et al. Gemma 3 technical report. arXiv preprint arXiv:2503.19786, 2025.
- Hyunmo Kang, Abdulkadir Canatar, and SueYeon Chung. Spectral analysis of representational similarity with limited neurons. arXiv preprint arXiv:2502.19648, 2025.
- John Kirchenbauer, Jonas Geiping, Yuxin Wen, Jonathan Katz, Ian Miers, and Tom Goldstein. A watermark for large language models. In International Conference on Machine Learning, pp. 17061-17084. PMLR, 2023.
- Simon Kornblith, Mohammad Norouzi, Honglak Lee, and Geoffrey Hinton. Similarity of neural network representations revisited. In *International conference on machine learning*, pp. 3519–3529. PMlR, 2019.
- Harold W Kuhn. The hungarian method for the assignment problem. *Naval research logistics quarterly*, 2(1-2):83-97, 1955.
- Erwan Le Merrer, Patrick Perez, and Gilles Trédan. Adversarial frontier stitching for remote neural network watermarking. Neural Computing and Applications (NCA), 32(13):9233-9244, 2020.
- Peixuan Li, Pengzhou Cheng, Fangqi Li, Wei Du, Haodong Zhao, and Gongshen Liu. Plmmark: a secure and robust black-box watermarking framework for pre-trained language models. In Proceedings of the AAAI Conference on Artificial Intelligence, volume 37, pp. 14991–14999, 2023.
- Zhouhan Lin, Minwei Feng, Cicero Nogueira dos Santos, Mo Yu, Bing Xiang, Bowen Zhou, and Yoshua Bengio. A structured self-attentive sentence embedding. *arXiv preprint arXiv:1703.03130*, 2017.
- Hanwen Liu, Zhenyu Weng, and Yuesheng Zhu. Watermarking deep neural networks with greedy residuals. In Proceedings of the International Conference on Machine Learning (ICML), pp. 6978–6988. PMLR, 2021.
- Nils Lukas, Yuxuan Zhang, and Florian Kerschbaum. Deep neural network fingerprinting by conferrable adversarial examples. arXiv preprint arXiv:1912.00888, 2019.
- Thomas Mesnard, Cassidy Hardin, Robert Dadashi, Surya Bhupatiraju, Shreya Pathak, Laurent Sifre, Morgane Rivière, Mihir Sanjay Kale, Juliette Love, et al. Gemma: Open models based on gemini research and technology. arXiv preprint arXiv:2403.08295, 2024.
- Alex Murphy, Joel Zylberberg, and Alona Fyshe. Correcting biased centered kernel alignment measures in biological and artificial neural networks. arXiv preprint arXiv:2405.01012, 2024.
- Xudong Pan, Yifan Yan, Mi Zhang, and Min Yang. Metav: A meta-verifier approach to task-agnostic model fingerprinting. In Proceedings of the 28th ACM SIGKDD Conference on Knowledge Discovery and Data Mining (SIGKDD), pp. 1327-1336, 2022.
- Guilherme Penedo, Quentin Malartic, Daniel Hesslow, Ruxandra Cojocaru, Alessandro Cappelli, Hamza Alobeidli, Baptiste Pannier, Ebtesam Almazrouei, and Julien Launay. The RefinedWeb dataset for Falcon LLM: outperforming curated corpora with web data, and web data only. arXiv preprint arXiv:2306.01116, 2023. URL https://arxiv.org/abs/2306.01116.
- Wenjun Peng, Jingwei Yi, Fangzhao Wu, Shangxi Wu, Bin Bin Zhu, Lingjuan Lyu, Binxing Jiao, Tong Xu, Guangzhong Sun, and Xing Xie. Are you copying my model? protecting the copyright of large language models for eaas via backdoor watermark. In Proceedings of the 61st Annual Meeting of the Association for Computational Linguistics (Volume 1: Long Papers), pp. 7653–7668, 2023.

- Zirui Peng, Shaofeng Li, Guoxing Chen, Cheng Zhang, Haojin Zhu, and Minhui Xue. Fingerprinting deep neural networks globally via universal adversarial perturbations. In Proceedings of the IEEE/CVF Conference on Computer Vision and Pattern Recognition (CVPR), pp. 13430-13439, 2022.
- pzc163 et al. Project author team stay tuned: I found out that the llama3-v project is stealing a lot of academic work from minicpm-llama3-v 2.5. github issue opened in the minicpm-o repository. https://github.com/OpenBMB/MiniCPM-o/issues/196, 2024. OpenBMB, June 2, 2024.
- Alec Radford, Karthik Narasimhan, Tim Salimans, Ilya Sutskever, et al. Improving language understanding by generative pre-training. 2018.
- Mark Russinovich and Ahmed Salem. Hey, that's my model! introducing chain & hash, an llm fingerprinting technique. arXiv preprint arXiv:2407.10887, 2024.
- Joseph P Simmons, Leif D Nelson, and Uri Simonsohn. False-positive psychology: Undisclosed flexibility in data collection and analysis allows presenting anything as significant. Psychological science, 22(11):1359-1366, 2011.
- Le Song, Alex Smola, Arthur Gretton, Karsten M Borgwardt, and Justin Bedo. Supervised feature selection via dependence estimation. In Proceedings of the 24th international conference on Machine learning, pp. 823-830, 2007.
- Jianlin Su, Murtadha Ahmed, Yu Lu, Shengfeng Pan, Wen Bo, and Yunfeng Liu. Roformer: Enhanced transformer with rotary position embedding. Neurocomputing, 568:127063, 2024.
- CodeGemma Team, Heri Zhao, Jeffrey Hui, Joshua Howland, Nam Nguyen, Siqi Zuo, Andrea Hu, Christopher A Choquette-Choo, Jingyue Shen, Joe Kelley, et al. Codegemma: Open code models based on gemma. arXiv preprint arXiv:2406.11409, 2024.
- InternLM Team. Internlm: A multilingual language model with progressively enhanced capabilities. https://github.com/InternLM/InternLM, 2023.
- Kimi Team, Yifan Bai, Yiping Bao, Guanduo Chen, Jiahao Chen, Ningxin Chen, Ruijue Chen, Yanru Chen, Yuankun Chen, Yutian Chen, et al. Kimi k2: Open agentic intelligence. arXiv preprint arXiv:2507.20534, 2025.
- Hugo Touvron, Thibaut Lavril, Gautier Izacard, Xavier Martinet, Marie-Anne Lachaux, Timothée Lacroix, Baptiste Rozière, Naman Goyal, Eric Hambro, Faisal Azhar, et al. Llama: Open and efficient foundation language models. arXiv preprint arXiv:2302.13971, 2023a.
- Hugo Touvron, Louis Martin, Kevin Stone, Peter Albert, Amjad Almahairi, Yasmine Babaei, Nikolay Bashlykov, Soumya Batra, Prajjwal Bhargava, Shruti Bhosale, et al. Llama 2: Open foundation and fine-tuned chat models. arXiv preprint arXiv:2307.09288, 2023b.
- Yusuke Uchida, Yuki Nagai, Shigeyuki Sakazawa, and Shin'ichi Satoh. Embedding watermarks into deep neural networks. In Proceedings of the 2017 ACM on International Conference on Multimedia Retrieval. ACM, jun 2017. doi: 10.1145/3078971.3078974. URL https://doi.org/10.1145% 2F3078971.3078974.
- Tianhao Wang and Florian Kerschbaum. Riga: Covert and robust white-box watermarking of deep neural networks. In Proceedings of the Web Conference 2021 (WWW), pp. 993–1004, 2021.
- Mengzhou Xia, Tianyu Gao, Zhiyuan Zeng, and Danqi Chen. Sheared llama: Accelerating language model pre-training via structured pruning. In The Twelfth International Conference on Learning Representations.

- Jiashu Xu, Fei Wang, Mingyu Ma, Pang Wei Koh, Chaowei Xiao, and Muhao Chen. Instructional fingerprinting of large language models. In Proceedings of the 2024 Conference of the North American Chapter of the Association for Computational Linguistics: Human Language Technologies (Volume 1: Long Papers), pp. 3277-3306, 2024.
- Kang Yang, Run Wang, and Lina Wang. Metafinger: Fingerprinting the deep neural networks with meta-training. In Proceedings of the International Joint Conference on Artificial Intelligence (IJCAI), 2022.
- Do-hyeon Yoon, Minsoo Chun, Thomas Allen, Hans Müller, Min Wang, and Rajesh Sharma. Intrinsic fingerprint of llms: Continue training is not all you need to steal a model! arXiv preprint arXiv:2507.03014, 2025.
- Boyi Zeng, Lizheng Wang, Yuncong Hu, Yi Xu, Chenghu Zhou, Xinbing Wang, Yu Yu, and Zhouhan Lin. Huref: Human-readable fingerprint for large language models. Advances in Neural Information Processing Systems, 37:126332-126362, 2024.
- Biao Zhang and Rico Sennrich. Root mean square layer normalization. Advances in neural information processing systems, 32, 2019.
- Jie Zhang, Dongrui Liu, Chen Qian, Linfeng Zhang, Yong Liu, Yu Qiao, and Jing Shao. REEF: Representation encoding fingerprints for large language models. In The Thirteenth International Conference on Learning Representations, 2025. URL https://openreview.net/forum?id=Sn DmPkOJOT.
- Susan Zhang, Stephen Roller, Naman Goyal, Mikel Artetxe, Moya Chen, Shuohui Chen, Christopher Dewan, Mona Diab, Xian Li, Xi Victoria Lin, et al. Opt: Open pre-trained transformer language models. arXiv preprint arXiv:2205.01068, 2022.
- Jingjing Zhao, Qingyue Hu, Gaoyang Liu, Xiaoqiang Ma, Fei Chen, and Mohammad Mehedi Hassan. Afa: Adversarial fingerprinting authentication for deep neural networks. Computer Communications, 150:488-497, 2020.
- Xuandong Zhao, Yu-Xiang Wang, and Lei Li. Protecting language generation models via invisible watermarking. In International Conference on Machine Learning, pp. 42187-42199. PMLR, 2023.
- Qinkai Zheng, Xiao Xia, Xu Zou, Yuxiao Dong, Shan Wang, Yufei Xue, Zihan Wang, Lei Shen, Andi Wang, Yang Li, Teng Su, Zhilin Yang, and Jie Tang. Codegeex: A pre-trained model for code generation with multilingual evaluations on humaneval-x. In KDD, 2023.

# A. Definitions and Notations

#### A.1. LLM Architecture

**Weights** Here we provide notations for the rest of model A's weights. In addition to the notations in section 3, we further denote s,  $W_{A,lm}$  as the language model head, and  $W_{A,V}^{(l)}, W_{A,O}^{(l)}, W_{A,ffn}^{(l)}$  the V,O matrices and FFN at the *l*-th layer, and

$$\begin{split} \mathbb{W}_{A,\text{others}} &= \mathbb{W}_A / \mathbb{W}_{A,\text{partial}} \\ &= \{W_{A,\text{lm}}\} \bigcup_{l=1}^L \mathbb{W}_{A,\text{ffn}}^{(l)} \bigcup_{l=1}^L \{W_{A,i}^{(l)} \mid i \in \{V,O\}\} \end{split}$$

as the rest of model A's weights.

Functions Here we provide definitions for functions in an LLM.

**Definition A.1** (RMSNorm). Given the input matrix  $X \in \mathbb{R}^{m \times n}$  of model A, the learnable parameters  $\omega_A^{(l)} = (\omega_{A,1}^{(l)}, \dots, \omega_{A,n}^{(l)}) \in \mathbb{R}^n$  at the l-th layer, and a constant  $\epsilon_A \in \mathbb{R}$  (this constant is usually shared across all layers of an LLM), RMSNorm at layer l is a function that

$$RMSNorm(X, \omega_A^{(l)}, \epsilon_A) = diag^{-\frac{1}{2}}(XX^{\mathsf{T}}\mathbf{1}_m + \epsilon_A\mathbf{1}_m) \cdot X \cdot diag(\omega_A^{(l)}). \tag{6}$$

**Definition A.2** (Self-Attention with RoPE). Given an input X to model A, the self-attention mechanism at layer l is a function  $f_{attn}$  that

$$f_{attn}^{(l)}(X) = AttnScore(X, W_{A,Q}^{(l)}, W_{A,K}^{(l)}, \theta) \cdot XW_{A,V}^{(l)\top} \cdot W_{A,Q}^{(l)\top}$$
(7)

where AttnScore is the attention score function with RoPE, i.e.

$$AttnScore(X, W_{A,Q}^{(l)}, W_{A,K}^{(l)}, \theta) = softmax\Big(\frac{1}{\sqrt{d}}RoPE(XW_{A,Q}^{(l)\top}, \theta) \cdot RoPE(XW_{A,K}^{(l)\top}, \theta)^{\top}\Big), \tag{8a}$$

$$RoPE(XW_{A,Q}^{(l)^{\top}}, \theta) = [x_1^{\top}W_{A,Q}^{(l)^{\top}}R_{\theta}(0), \dots, x_m^{\top}W_{A,Q}^{(l)^{\top}}R_{\theta}(m-1)],$$
(8b)

$$RoPE(XW_{A,K}^{(l)\top}, \theta) = [x_1^\top W_{A,K}^{(l)\top} R_{\theta}(0), \dots, x_m^\top W_{A,K}^{(l)\top} R_{\theta}(m-1)].$$
(8c)

Here  $x_i^{\top} \in \mathbb{R}^n$  is the i-th row of X,  $\theta$  is the frequency base for RoPE and  $R_{\theta}$  is the rotation matrix (Su et al., 2024).

RoPE's definition in Definition A.2 is slightly different from their implementations, but still an equivalent version to Su et al. (2024).

**Definition A.3** (Feed-forward Networks). Given the input X, the feed-forward network which adopts the SwiGLU MLP is the function  $f_{ffn}^{(l)}$  defined by

$$f_{ffn}^{(l)}(X) = \left(SiLU(XW_{A,gate}^{(l)\top}) \odot \left(XW_{A,up}^{(l)\top}\right)\right)W_{A,down}^{(l)\top},$$

where  $W_{A,up}^{(l)}$ ,  $W_{A,gate}^{(l)}$ ,  $W_{A,down}^{(l)}$  are bias-free weight matrices,  $\odot$  denotes the Hadamard product, and  $SiLU(z)=z\,\sigma(z)$  with  $\sigma(z)=\frac{1}{1+e^{-z}}$ . We write  $\mathbb{W}_{A,ffn}^{(l)}=\left\{W_{A,up}^{(l)},\,W_{A,gate}^{(l)},\,W_{A,down}^{(l)}\right\}$ .

We abuse the notations in Definition A.1 by denoting RMSNorm $^{(l)}_{attn}(X) \triangleq RMSNorm(X, \omega^{(l)}_{A,attn}, \epsilon_A)$  as the attention norm and RMSNorm $^{(l)}_{ffn}(X) \triangleq RMSNorm(X, \omega^{(l)}_{A,ffn}, \epsilon_A)$  the ffn norm at layer l of model A. Then, the definition of a Transformer block at layer l of model A can be summartized as follows.

**Definition A.4** (Transformer Block). Combining all the components with residual connections, the transformer block at the l-th layer of model A is a function  $f_{Transformer}^{(l)}$  that

$$f_{Transformer}^{(l)} = \left(I + f_{ffn}^{(l)} \circ RMSNorm_{ffn}^{(l)}\right) \circ \left(I + f_{attn}^{(l)} \circ RMSNorm_{attn}^{(l)}\right). \tag{9}$$

where I is the identity mapping,  $f_{attn}^{(l)}$  and  $f_{ffn}^{(l)}$  are the attention and FFN at l-th layer respectively,  $RMSNorm_{ffn}^{(l)}$  and  $RMSNorm_{attn}^{(l)}$  are RMSNorm functions for these two components.

**Definition A.5** (LLM Architecture). *Given an word embedding X, the last hidden state Y of an L-layered LLM A is* 

$$Y = f_{Transformer}^{(L)} \circ f_{Transformer}^{(L-1)} \circ \cdots \circ f_{Transformer}^{(L-1)}(X) \cdot W_{A,lm}^{\top}.$$
 (10)

# A.2. Central Kernel Alignment (CKA)

Given two input matrices  $X_1 \in \mathbb{R}^{m \times n_1}$  and  $X_2 \in \mathbb{R}^{m \times n_2}$ , CKA is a function mapping paired input matrices to [0, 1], and

$$CKA(X_1, X_2) = \frac{HSIC(K_{X_1}, K_{X_2})}{\sqrt{HSIC(K_{X_1}, K_{X_1}) \cdot HSIC(K_{X_2}, K_{X_2})}}$$
(11)

where  $\operatorname{HSIC}(K_{X_1}, K_{X_2}) = \frac{1}{(m-1)^2} \operatorname{tr}(K_{X_1} H_m K_{X_2} H_m)$ ,  $(K_{X_1})_{ij} = k((X_1)_i, (X_1)_j)$ ,  $(K_{X_2})_{ij} = k((X_2)_i, (X_2)_j)$  are kernel matrices with the kernel function  $k(\cdot, \cdot) : \mathbb{R}^m \times \mathbb{R}^m \to \mathbb{R}_+$ , and  $H_m = I_m - \frac{1}{m} \mathbf{1}_m \mathbf{1}_m^\top$  is the centering matrix. The linear kernels give  $K_X = XX^\top$  for a matrix X. To reduce the finite-sample bias of Eq. (6), we use the unbiased HSIC estimator (Song et al., 2007). Let  $\tilde{K}_{X_i}$  be  $K_{X_i}$  with its diagonal set to zero, i.e.,  $(\tilde{K}_{X_i})_{ii} = 0$ . With  $\mathbf{1}_m$  the all-ones vector of length m, the unbiased HSIC is

$$HSIC_{u}(\tilde{K}_{X_{1}}, \tilde{K}_{X_{2}}) = \frac{1}{m(m-3)} \left[ tr(\tilde{K}_{X_{1}} \tilde{K}_{X_{2}}) + \frac{(1_{m}^{\top} \tilde{K}_{X_{1}} 1_{m})(1_{m}^{\top} \tilde{K}_{X_{2}} 1_{m})}{(m-1)(m-2)} - \frac{2}{m-2} 1_{m}^{\top} \tilde{K}_{X_{1}} \tilde{K}_{X_{2}} 1_{m} \right].$$
(12)

We then define

$$UCKA(X_1, X_2) = \frac{HSIC_u(\tilde{K}_{X_1}, \tilde{K}_{X_2})}{\sqrt{HSIC_u(\tilde{K}_{X_1}, \tilde{K}_{X_1}) \cdot HSIC_u(\tilde{K}_{X_2}, \tilde{K}_{X_2})}},$$
(13)

which preserves Theorem 3.1 and yields values in [-1, 1].

# **B.** Proofs and Discussions

#### **B.1. Proof for Theorem 3.1**

We give the proof based on the definition of CKA with linear kernels in Appendix A.2. Given input matrices  $X_1, X_2$ , orthogonal matrices  $U_1, U_2$  and constants  $c_1, c_2$ , the kernel functions yield

$$\begin{split} K_{c_1X_1U_1} &= c_1X_1U_1U_1^{\top}X_1^{\top}c_1 = c_1^2X_1X_1^{\top} = c_1^2K_{X_1}, \\ K_{c_2X_2U_2} &= c_2X_2U_2U_2^{\top}X_2^{\top}c_2 = c_2^2X_2X_2^{\top} = c_2^2K_{X_2}. \end{split}$$

Therefore, corresponding HSIC results are

$$\begin{aligned} & \operatorname{HSIC}(K_{c_1X_1U_1}, K_{c_2X_2U_2}) = \frac{c_1^2c_2^2}{(m-1)^2} \operatorname{tr}(K_{X_1}H_mK_{X_2}H_m) = c_1^2c_2^2 \operatorname{HSIC}(K_{X_1}, K_{X_2}), \\ & \operatorname{HSIC}(K_{c_1X_1U_1}, K_{c_1X_1U_1}) = \frac{c_1^4}{(m-1)^2} \operatorname{tr}(K_{X_1}H_mK_{X_1}H_m) = c_1^4 \operatorname{HSIC}(K_{X_1}, K_{X_1}), \\ & \operatorname{HSIC}(K_{c_2X_2U_2}, K_{c_2X_2U_2}) = \frac{c_2^4}{(m-1)^2} \operatorname{tr}(K_{X_2}H_mK_{X_2}H_m) = c_2^4 \operatorname{HSIC}(K_{X_2}, K_{X_2}). \end{aligned}$$

Hence, it follows that

$$\begin{split} \mathsf{CKA}(c_1X_1U_1,c_2X_2U_2) &= \frac{\mathsf{HSIC}(K_{c_1X_1U_1},K_{c_2X_2U_2})}{\sqrt{\mathsf{HSIC}(K_{c_1X_1U_1},K_{c_1X_1U_1}) \cdot \mathsf{HSIC}(K_{c_2X_2U_2},K_{c_2X_2U_2})}} \\ &= \frac{c_1^2c_2^2\mathsf{HSIC}(K_{X_1},K_{X_2})}{c_1^2c_2^2\sqrt{\mathsf{HSIC}(K_{X_1},K_{X_1}) \cdot \mathsf{HSIC}(K_{X_2},K_{X_2})}} \\ &= \frac{\mathsf{HSIC}(K_{X_1},K_{X_2})}{\sqrt{\mathsf{HSIC}(K_{X_1},K_{X_1}) \cdot \mathsf{HSIC}(K_{X_2},K_{X_2})}} \\ &= \mathsf{CKA}(X_1,X_2). \end{split}$$

# **B.2. Proof for Proposition 4.2**

The goal is to show the manipulation T commutes with f, i.e.  $f \circ T = T \circ f$ . If  $f = f_n \circ \cdots \circ f_1$ , then it suffices to show

$$f_n \circ \cdots \circ f_1 \circ T = T \circ f_n \circ \ldots f_1.$$

Since

$$f_1 \circ T = T \circ f_1, f_2 \circ T = T \circ f_2, \dots, f_n \circ T = T \circ f_n,$$

It is direct that

$$f \circ T = T \circ f$$
.

# B.3. Proof for Theorem 4.3 and Discussions on Other Input Manipulations

We first show a proof for the claims in Theorem 4.3. The core lies in preserving the diagonal structure of RMSNorm parameters in Definition A.1. Given the input X to layer I, the manipulations change it to cXPD and fed the manipulated input into the attention norm of model B. In order to recover the manipulations on inputs after RMSNorm, i.e. for any manipulation T in the input X (an example is T(X) = cXPD),

$$RMSNorm_{attn}^{(l)} \circ T = T \circ RMSNorm_{attn}^{(l)}, \tag{14}$$

it suffices to show

$$\exists \omega_{B, \text{attn}}^{(l)} \text{ and } \epsilon_B, \text{ s.t. RMSNorm}(X, \omega_{A, \text{attn}}^{(l)}, \epsilon_A) \cdot cPD = \text{RMSNorm}(cXPD, \omega_{B, \text{attn}}^{(l)}, \epsilon_B)$$

since the learnable parameters and norm epsilon can be modified to satisfy Equation 14 and Proposition 4.2. By setting  $\epsilon_B = c^2 \epsilon_A$  and  $\operatorname{diag}(\omega_{B,\operatorname{attn}}^{(l)}) = cD^\top P^\top \operatorname{diag}(\omega_{A,\operatorname{attn}}^{(l)}) PD$ , one has

$$\begin{split} & \operatorname{RMSNorm}(cXPD, \omega_{B, \operatorname{attn}}^{(l)}, \epsilon_B) \\ &= \operatorname{diag}^{-\frac{1}{2}} \left( (cXPD)(cXPD)^{\top} \mathbf{1}_m + \epsilon_B \mathbf{1}_m \right) \cdot cXPD \cdot \operatorname{diag}(\omega_{B, \operatorname{attn}}^{(l)}) \\ &= \operatorname{diag}^{-\frac{1}{2}} (c^2XX^{\top} \mathbf{1}_m + c^2 \epsilon_A \mathbf{1}_m) \cdot cXPD \cdot cD^{\top} P^{\top} \operatorname{diag}(\omega_{A, \operatorname{attn}}^{(l)}) PD \\ &= c \cdot \operatorname{diag}^{-\frac{1}{2}} (XX^{\top} \mathbf{1}_m + \epsilon_A \mathbf{1}_m) \cdot X \cdot \operatorname{diag}(\omega_{A, \operatorname{attn}}^{(l)}) \cdot PD \\ &= \operatorname{RMSNorm}(X, \omega_{A, \operatorname{attn}}^{(l)}) \cdot cPD. \end{split}$$

The proof still holds for partial permutations P, i.e. P is rectangular with number of rows more than number of columns, since  $cD^{\top}P^{\top}\mathrm{diag}(\omega_{A,\mathrm{attn}}^{(l)})PD$  is still a diagonal matrix. Therefore,  $R_{B,\mathrm{emb}} = cPD$  under Proposition 4.2. However, for more general manipulations, Proposition 4.2 does not hold for RMSNorm. We give two examples for illustration.

First, orthogonal transformations on the input generally fail to pass through RMSNorm. Given any orthogonal matrices U as the manipulation on X, i.e., T(X) = XU, if one attempts to keep Equation 14, then it requires

$$\exists \omega^{(l)} \text{ and } \epsilon, \text{ s.t. RMSNorm}(XU, \omega^{(l)}, \epsilon) = \text{RMSNorm}(X, \omega^{(l)}_{A, \text{attn}}, \epsilon_A)U.$$

However,

RMSNorm
$$(XU, \omega, \epsilon) = \operatorname{diag}^{-\frac{1}{2}}(XX^{\mathsf{T}}\mathbf{1}_m + \epsilon\mathbf{1}_m) \cdot XU \cdot \operatorname{diag}(\omega^{(l)}).$$

Hence, it is required that

$$U \cdot \operatorname{diag}(\omega^{(l)}) = \operatorname{diag}(\omega_{A,\text{attn}}^{(l)})U$$

which suggests  $U^{\mathsf{T}}\mathrm{diag}(\omega_{A,\mathrm{attn}}^{(l)})U$  is a diagonal matrix. Nevertheless, this property generally does not hold if U is not a (partial) permutation matrix P or a signature matrix D.

Second, non-orthogonal transformations on inputs generally fail to pass through RMSNorm. Given an arbitrary (invertible) transformation *M*, Proposition 4.2 and Equation 14 require that

$$\exists \omega^{(l)} \text{ and } \epsilon, \text{ s.t. RMSNorm}(XM, \omega^{(l)}, \epsilon) = \text{RMSNorm}(X, \omega^{(l)}_{A, \text{attn}}, \epsilon_A)M.$$

However, since

RMSNorm
$$(XM, \omega^{(l)}, \epsilon) = \operatorname{diag}^{-\frac{1}{2}}(XMM^{\top}X^{\top}\mathbf{1}_m + \epsilon\mathbf{1}_m) \cdot XM \cdot \operatorname{diag}(\omega^{(l)}),$$

any M that do not satisfy  $MM^{\top} = c'I$  where c' is a constant and I is the identity matrix can hardly recover the manipulations due to the nonlinearity in norm functions. Moreover, similar to the case with orthogonal transformations,  $M \cdot \operatorname{diag}(\omega^{(l)}) = \operatorname{diag}(\omega^{(l)}_{A,\operatorname{attn}})M$  also requires M to be (partial) permutation or signature matrices (or a combination of the both).

Third, we additionally clarify that although the combination of (partial) permutation and signature matrices can be in any order, it is reasonable to fix it as  $R_{B,emb} = cPD$ . To be specific, we clarify that for any (partial) permutation matrix P' and signature matrix D', there exists a (partial) permutation matrix P and a signature D such that

$$D'P' = PD$$

The proof is straightforward. Define P entry-wise by

$$P_{ij} := |(D'P')_{ij}| \in \{0, 1\}.$$

Since left-multiplication by D' only flips signs, each column of D'P' has at most one nonzero entry. Hence, P is a partial permutation matrix. For each column j, if that column of D'P' has its unique nonzero at row i, set

$$D_{jj} := \operatorname{sgn}((D'P')_{ij}) \in \{\pm 1\}.$$

If the column is entirely zero, choose  $D_{ij} \in \{\pm 1\}$  arbitrarily. Then for all i, j,

$$(PD)_{ij} = P_{ij}D_{jj} = |(D'P')_{ij}| \cdot \text{sgn}((D'P')_{ij}) = (D'P')_{ij},$$

where we interpret sgn(0) = 1. Therefore, PD = D'P'.

Last, we clarify that the conclusions in Theorem 4.3 can generalize to the case where model A and model B may not share the same architecture. It is a direct result from the fact that the two LLMs have shared tokens and that the pruning over dimensions of a model's word embeddings can be viewed as a partial permutation matrix.

## B.4. Proof for Theorem 4.4 and Related Discussions

We first provide the proof for Theorem 4.4 based on Definition A.2.

We denote by X the original input to self-attention, and X' the manipulated one. Then, Theorem 4.3 suggests that

$$X' = cXPD$$

Therefore, the attention score of model B becomes

$$\operatorname{AttnScore}(cXPD, W_{B,Q}^{(l)}, W_{B,K}^{(l)}, \theta) = \operatorname{softmax} \left( \frac{1}{\sqrt{d}} \operatorname{RoPE}(cXPDW_{B,Q}^{(l)\top}, \theta) \cdot \operatorname{RoPE}(cXPDW_{B,K}^{(l)\top}, \theta)^{\top} \right).$$

To keep attention scores of model B identical to that of model A, it is required that

$$\mathsf{ROPE}(cXPDW_{B,Q}^{(l)\top},\theta) \cdot \mathsf{ROPE}(cXPDW_{B,K}^{(l)\top},\theta)^\top = \mathsf{ROPE}(XW_{A,Q}^{(l)\top},\theta) \cdot \mathsf{ROPE}(XW_{A,K}^{(l)\top})^\top.$$

By Equation 8b and Equation 8c, this translates into

$$c^2 x_i^{\mathsf{T}} P D W_{B,O}^{(l)\mathsf{T}} R_{\theta}(i) R_{\theta}^{\mathsf{T}}(j) W_{B,K}^{(l)} D^{\mathsf{T}} P^{\mathsf{T}} x_j = x_i^{\mathsf{T}} W_{A,O}^{(l)\mathsf{T}} R_{\theta}(i) R_{\theta}^{\mathsf{T}}(j) W_{A,K}^{(l)} x_j$$

Therefore, the recovery of model A's attention score requires column-wise transformations to eliminate the **input-related manipulations passed by RMSNorm**, i.e.

$$W_{B,O}^{(l)} = c^{-1}W_{A,O}^{(l)}PD, \quad W_{B,K}^{(l)} = c^{-1}W_{A,K}^{(l)}PD$$
 (15)

which suggests

$$R_{B,O}^{(l)} = R_{B,K}^{(l)} = c^{-1}PD.$$

Although Equation 15 recovers attention scores, the Q,K matrices can still be modified without changing attention scores. An example is, given a rotation matrix  $R = R_{\theta}(k)$  with the same frequency base as RoPE, multiplying Q,K matrices with it does not change the attention scores, i.e.

$$\begin{split} x_i^\top W_{B,Q}^{(l)\top} R_\theta(k) R_\theta(i) R_\theta^\top(j) R_\theta^\top(k) W_{B,K}^{(l)} x_j &= x_i^\top W_{B,Q}^{(l)\top} R_\theta(i+k) R_\theta^\top(j+k) W_{B,K}^{(l)\top} x_j \\ &= x_i^\top W_{B,Q}^{(l)\top} R_\theta(i-j) W_{B,K}^{(l)} x_j \\ &= x_i^\top W_{B,Q}^{(l)\top} R_\theta(i) R_\theta^\top(j) W_{B,K}^{(l)\top} x_j. \end{split}$$

Furthermore, this conclusion can be generalize to any rotation matrix with structures similar to RoPE rotation matrices. Given  $R = \operatorname{diag}(R(\psi_0), R(\psi_1), \dots)$  with  $R(\psi_k) = \begin{bmatrix} \cos \psi_k & -\sin \psi_k \\ \sin \psi_k & \cos \psi_k \end{bmatrix}$ , multiplying Q,K matrices by R keeps the attention scores since

$$RR_{\theta}(i)R_{\theta}^{\top}(j)R^{\top} = R_{\theta}(i)R_{\theta}^{\top}(j). \tag{16}$$

Hence, there are various rotation matrices to significantly change Q,K matrices but preserve attention scores. Since these rotation matrices are naturally orthogonal, we reformulate the row-wise transformations on Q,K matrices  $L_{B,Q}$ ,  $L_{B,K}$  as  $U_{B,Q}^{(l)}$  and  $U_{B,K}^{(l)}$ .

Therefore, we denote RoPE-related manipulations as

$$W_{B,Q}^{(l)} = U_{A,Q}^{(l)} W_{B,Q}^{(l)}, \quad W_{B,K}^{(l)} = U_{A,K}^{(l)} W_{B,K}^{(l)}.$$

On the other hand, semi-orthogonal  $U_{B,Q}^{(l)}, U_{B,K}^{(l)}$  are also possible. This is because of the common practice in pruning may select different different rows of Q,K matrices, which suggests multiplying Q,K matrices with row-wise partial permutations.

Next, we show how Proposition 4.2 is satisfied at the self-attention mechanism based on Theorem 4.4. Let  $W_{B,V}^{(l)} = W_{A,V}^{(l)} PD$  and  $W_{B,O}^{(l)} = D^{\top} P^{\top} W_{A,O}^{(l)}$ . Then,

$$\begin{aligned} X'W_{B,\mathbf{V}}^{(l)\top}W_{B,\mathbf{O}}^{(l)\top} &= cXPD \cdot D^{\top}P^{\top}W_{A,\mathbf{V}}^{(l)\top}W_{A,\mathbf{O}}^{(l)\top}PD \\ &= XW_{A,\mathbf{V}}^{(l)\top}W_{A,\mathbf{O}}^{(l)\top} \cdot cPD \end{aligned}$$

recovers the manipulation over inputs in Equation 7.

# B.5. How Potential Attacks in subsection 4.5 Recovers the Output of Transformers

We provide an illustration based on Definition A.3, Definition A.4 and Definition A.5. Previous parts have demonstrated how the manipulations on inputs pass through self-attention. Hence, it suffices to show how the manipulations pass through FFN and yield an output identical to model A after the language model head.

For layer l, let  $W_{B,\mathrm{gate}}^{(l)} = c^{-1}W_{A,\mathrm{gate}}^{(l)}PD$ ,  $W_{B,\mathrm{gate}}^{(l)} = c^{-1}W_{A,\mathrm{gate}}^{(l)}PD$ ,  $W_{B,\mathrm{down}}^{(l)} = cD^{\top}P^{\top}W_{A,\mathrm{down}}^{(l)}$ . We denote X' = cXPD as the manipulated input. Then for model B,

$$\begin{split} &f_{\text{ffn}}^{(l)}(X') \\ &= \left( \text{SiLU} \big( X' W_{B,\text{gate}}^{(l) \top} \big) \odot \big( X' W_{B,\text{up}}^{(l) \top} \big) \right) W_{B,\text{down}}^{(l) \top} \\ &= \left( \text{SiLU} \big( c X P D \cdot D^{\top} P^{\top} W_{A,\text{gate}}^{(l) \top} \cdot c^{-1} \big) \odot \big( c X P D \cdot D^{\top} P^{\top} W_{A,\text{up}}^{(l) \top} \cdot c^{-1} \big) \right) W_{B,\text{down}}^{(l) \top} \cdot c P D \\ &= \left( \text{SiLU} \big( X W_{A,\text{gate}}^{(l) \top} \big) \odot \big( X W_{A,\text{up}}^{(l) \top} \big) \right) W_{A,\text{down}}^{(l) \top} \cdot c P D. \end{split}$$

By Definition A.4 and Definition A.5, the manipulation is propagated through transformer layers. At the language model head, we denote  $W_{B,\text{lm}} = c^{-1}W_{A,\text{lm}}PD$  and abuse X' = cXPD as the manipulated input. Then,

$$\begin{split} X'W_{B,\mathrm{lm}}^{(l)\top} &= cXPD \cdot D^{\top}P^{\top}W_{A,\mathrm{lm}}^{(l)\top} \cdot c^{-1} \\ &= XW_{A,\mathrm{lm}}^{(l)\top} \end{split}$$

recovers the output of model A.

# C. Mapping of Model abbreviations

Table 4 details the mapping between the abbreviations used throughout the paper, their respective base models, and their full model names as cataloged on the Hugging Face Hub.

**Table 4** | Mapping of model abbreviations to their full Hugging Face model names.

Base Model	Full Model Name
Llama2-7B	vicuna-7b-v1.5
Llama2-7B	llama-2-7b-finance
Llama2-7B	selfrag_llama2_7b
Llama2-7B	LLaMA-2-7B-32K
Llama2-7B	WizardMath-7B-V1.0
Llama2-13B	llama-2-7b-guanaco
Llama2-13B	vicuna-13b-v1.5
Llama2-13B	Nous-Hermes-Llama2-13b
Llama2-13B	LLaMA2-13B-Estopia
Llama2-13B	firefly-llama2-13b
Llama2-7B	llemma 7b
Llama2-7B	CodeLlama-7b-hf
Llama2-7B	CodeLlama-7b-Python-hf
Gemma-2B	codegemma-2b
Gemma-7B	codegemma-7b
Qwen2.5-7B	Qwen2.5-Math-7B
-	Qwen2.5-Coder-7B
Qwen2-7B	Qwen2-Math-7B
Llama2-70B	CodeLlama-70b-hf
Llama2-70B	CodeLlama-70b-Python-hf
Mistral-7B	Nous-Hermes-2-Mixtral-8x7B-DPO
	LLaMA-MoE-v2-3 8B-2 8-sft
	LLaMA-MoE-v1-3 5B-4 16
Llama2-7B	LLaMA-MoE-v1-3 0B-2 16
	LLaMA-MoE-v1-3 5B-2 8
	LLaMA-MoE-v1-3 0B-2 16-sft
	LLaMA-MoE-v1-3 5B-2 8-sft
	LLaMA-MoE-v1-3 5B-4 16-sft
Owen-1.8B	Qwen1.5-MoE-A2.7B
Minicpm-2B	MiniCPM-MoE-8x2B
Llama2-7B	llava-v1.5-7b
Llama2-7B	Video-LLaVA-7B-hf
Qwen2-7B	Qwen2-VL-7B-Instruct
-	Owen-Audio
-	Qwen2-Audio-7B
-	Qwen-VL
-	Qwen2.5-VL-7B-Instruct
_	Qwen2.5-VL-3B-Instruct
Llama3-8B	llama3-llava-next-8b-hf
	Llama2-7B Llama2-7B Llama2-7B Llama2-7B Llama2-7B Llama2-13B Llama2-13B Llama2-13B Llama2-13B Llama2-13B Llama2-13B Llama2-7B Llama2-7B Llama2-7B Llama2-7B Llama2-7B Qwen2.5-7B Qwen2.5-7B Qwen2.5-7B Llama2-70B Llama2-70B Llama2-70B Llama2-7B Qwen-1.8B Minicpm-2B Llama2-7B Qwen-7B



Table 4 – continued from previous page

Abbreviation	Base Model	Full Model Name
LLaVA	Llama2-13B	llava-v1.5-13b
RLHF	Open-llama3B	hh_rlhf_rm_open_llama_3b
Reason	Qwen2.5-7B	Nemotron-Research-Reasoning-Qwen-1.5B
Zero	Qwen2.5-1.5B	Open-Reasoner-Zero-1.5B
DPO	Mixtral	Nous-Hermes-2-Mixtral-8x7B-DPO
DPO	Mistral-7B	Nous-Hermes-2-Mistral-7B-DPO
Dolphin	Mistral-7B	dolphin-2.6-mistral-7b-dpo
DPO	Minicpm-2B	MiniCPM-2B-dpo-bf16
GRPO	Qwen3-4B	Qwen3_Medical_GRPO
RLHF	Chatglm-6B	chatglm-fitness-RLHF
DPO	Llama3-8B	LLaMA3-iterative-DPO-final
Minitron-Depth	Llama-3-8B	Llama-3.1-Minitron-4B-Depth-Base
Minitron-Width	Llama-3-8B	Llama-3.1-Minitron-4B-Width-Base
Llama3-1B	Llama3-8B	Llama-3.2-1B
Llama3-3B	Llama3-8B	Llama-3.2-3B
Sheared 2.7B-P	Llama2-7B	Sheared-LLaMA-2.7B-Pruned
Sheared 2.7B-S	Llama2-7B	Sheared-LLaMA-2.7B-ShareGPT
Sheared 2.7B	Llama2-7B	Sheared-LLaMA-2.7B
Sheared 1.3B-P	Llama2-7B	Sheared-LLaMA-1.3B-Pruned
Sheared 1.3B	Llama2-7B	Sheared-LLaMA-1.3B
Sheared 1.3B-S	Llama2-7B	Sheared-LLaMA-1.3B-ShareGPT